Effects of Aquatic Vegetation on Gas Exchange Process Across Air-Water and Sediment-Water Interface

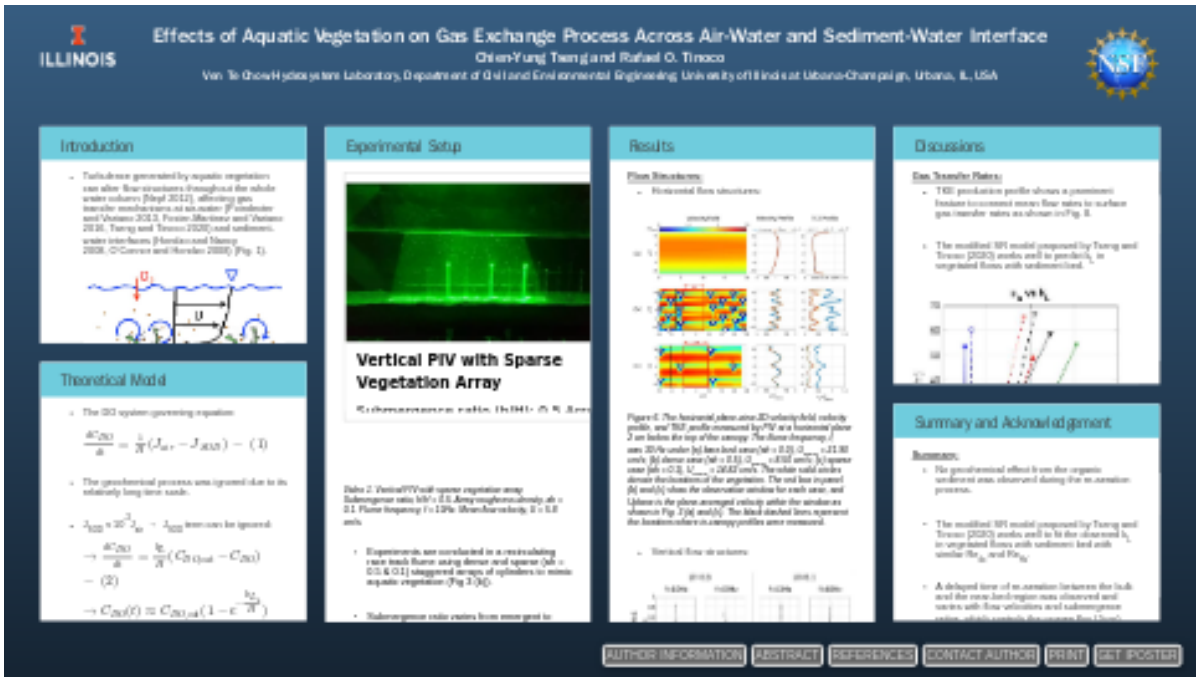

Chien-Yung Tseng and Rafael O. Tinoco

Ven Te Chow Hydrosystem Laboratory, Department of Civil and Environmental Engineering, University of Illinois at Urbana-Champaign, Urbana, IL, USA

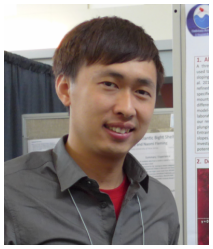

PRESENTED AT:

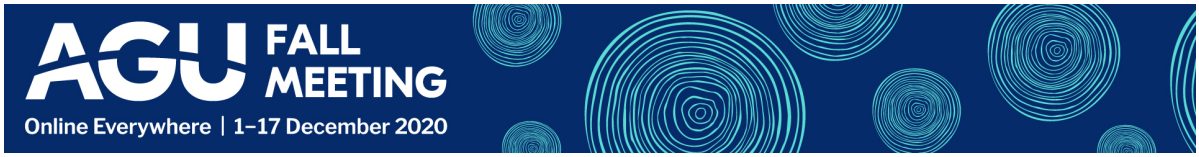

INTRODUCTION

- A quick guide to the poster:

[VIDEO] https://www.youtube.com/embed/ARpkCf4-mMA?rel=0&fs=1&modestbranding=1&rel=0&showinfo=0

- Turbulence generated by aquatic vegetation can alter flow structures throughout the whole water column (Nepf 2012), affecting gas transfer mechanisms at air-water (Poindexter and Variano 2013, Foster-Martinez and Variano 2016, Tseng and Tinoco 2020) and sediment-water interfaces (Hondzo and Nancy 2008, O'Connor and Hondzo 2008) (Fig. 1).

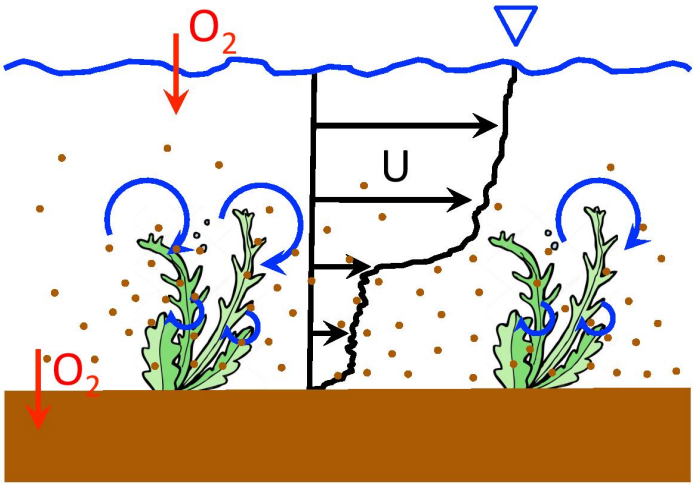

Figure 1. Sketch of the gas transfer process across air-water and sediment-water interfaces in vegetated flows.

- A series of laboratory experiments were conducted with arrays of acrylic cylinders to mimic the aquatic vegetation in a recirculating race-track flume.

- Particle Image Velocimetry (PIV) was conducted for flow characterization within and above the array.

- Gas transfer rates across air-water and sediment-water interfaces were determined by monitoring the dissolved oxygen (DO) concentration during the re-aeration process near the surface and the bed.

- Our data shows that no geochemical effect from the organic sediment was observed during the re-aeration process.

- The modified surface renewal (SR) model proposed by Tseng and Tinoco (2020) was applied to compare the observed surface gas transfer rates in vegetated flows with the sediment bed.

- A delayed time of re-aeration between the water and the near-bed region was observed.

THEORETICAL MODEL

- The DO system governing equation:

$$\frac{dC_{DO}}{dt} = \frac{1}{H}(J_{air} - J_{SOD}) \ - \ (1)$$

- The geochemical process was ignored due to its relatively long time scale.

- $J_{SOD} \approx 10^{-3} J_{air} \rightarrow J_{SOD}$ term can be ignored:

$$\rightarrow \frac{dC_{DO}}{dt} = \frac{k_L}{H}(C_{DO,sat} - C_{DO}) \ - \ (2) \rightarrow C_{DO}(t) \approx C_{DO,sat}(1 - e^{-\frac{k_L}{H}t}) \ - \ (3)$$

- J_{SOD} flux can be estimated following Voermans et al., 2018:

$$J_{SOD} = -D_{eff}\theta_p \frac{dC_{DO}}{dz} \ - \ (4)$$
$$\rightarrow \frac{dC_{DO}}{dz} \approx \frac{C_{DO} - C_{DO,b}}{\delta_c} \ - \ (5)$$

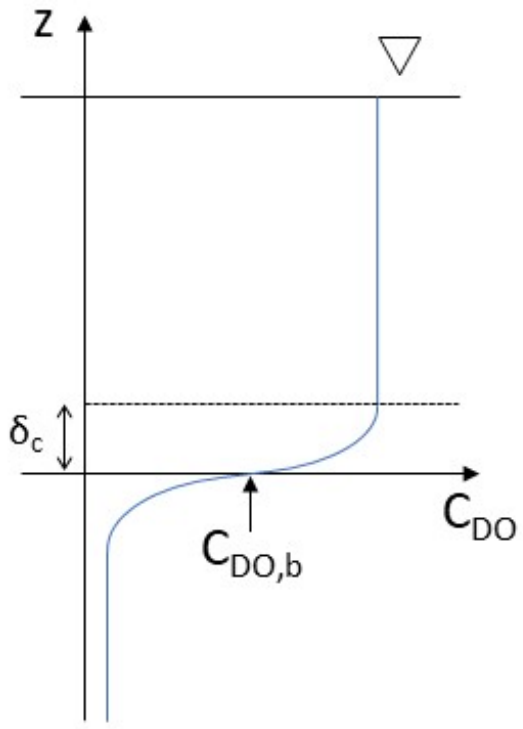

Figure 2. Sketch of the DO concentration profile and the defined diffusive-sublayer thickness, δ_c .

- The re-aeration process dominates the DO dynamics near the surface and the bed, but a delayed time can be observed in our cases:

$$C_{DO} - C_{DO,b} = C_{DO,sat}[(1 - e^{-\frac{k_L}{H}t}) - (1 - e^{-\frac{k_L}{H}(t-\Delta t)})] = C_{DO,sat}e^{-\frac{k_L}{H}t}[(e^{\frac{k_L}{H}\Delta t} - 1) \ - \ (6)$$

- Symbol representation:

  C_{DO} : bulk DO concentration

  $C_{DO,sat}$: saturated DO concentration

  CDO,b : near-bed DO concentration

  J_{air} : DO flux from air to water

  J_{sod} : DO flux from water to sediment

  H : water depth

  θ_p : sediment porosity

  k_L : surface gas transfer rate

  D_{eff} : effective diffusivity

  δ_c : diffusive-sublayer thickness

EXPERIMENTAL SETUP

Video 1. Vertical PIV with sparse vegetation array. Submergence ratio, h/H = 0.5. Array roughness density, ah = 0.1. Flume frequency, f = 10Hz. Mean flow velocity, U = 5.8 cm/s.

- Experiments are conducted in a recirculating race track flume using dense and sparse (ah = 0.5 & 0.1) staggered arrays of cylinders to mimic aquatic vegetation (Fig 3 (b)).

- Submergence ratio varies from emergent to fully submerged arrays, h/H={1, 0.5, 0.25}.

- A frequency controlled (10 - 40 Hz) disk pump drives the flow for a velocity range U = {2 − 25} cm/s yielding Re_d = {100 − 600}, Re_H = {300 − 8,000}.

- 2 D PIV was used to characterize the vertical and the horizontal flow field (Fig 3 (d)). PIV: 5W continuous wave Laser and 5MP JAI camera (60fps) (Fig. 4 (a)).

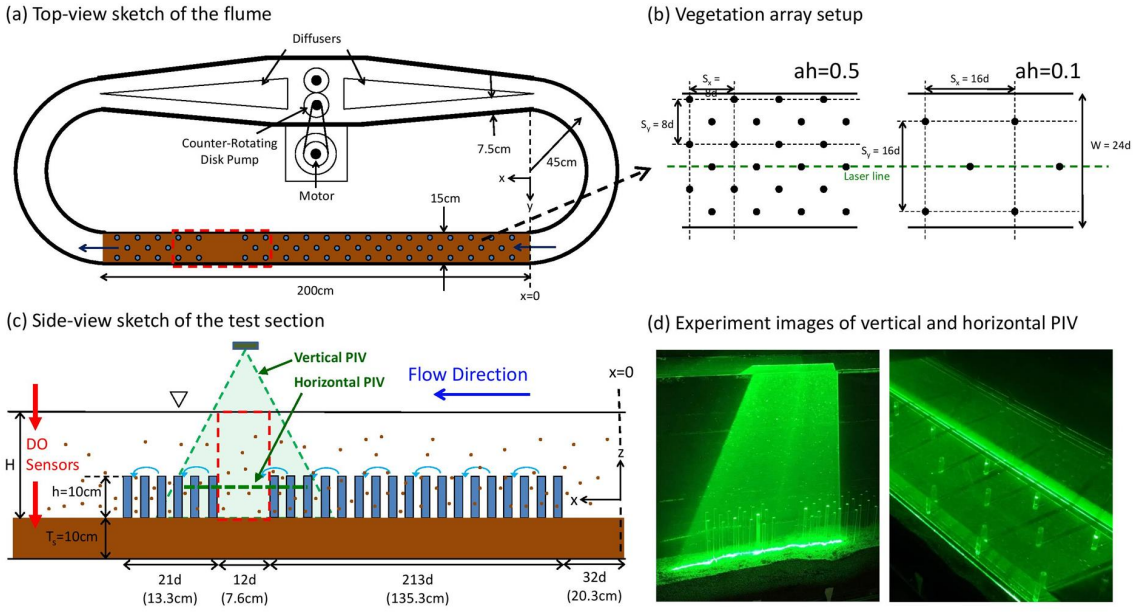

Figure 3. Sketch of the recirculating racetrack flume (not to scale). (a) Top view sketch of the flume and (c) side view of the straight test section. (b) Staggered grid configuration of the dense (ah=0.5) and sparse (ah=0.1) arrays. (d) The experimental images of vertical and horizontal PIV.

- Sodium Sulfite (Na_2SO_3) was put into water as an oxygen depletion agent. Two PASCO optical DO sensors (Fig. 4 (b)) were located near the surface and the bed (Fig. 5 (b)) to record DO concentration during the re-aeration process.

Figure 4. (a) 5-Megapixel CCD Camera, JAI GO-5000M-USB3, and (b) PASPORT Optical Dissolved Oxygen Sensor, PASCO.

- Crushed walnut shell was chosen as the sediment substrate due to its light-weight characteristics (ρ_s = 1.2g/cm^3) to account for the sediment dynamics scaling in the laboratory experiment (Fig 5 (a)). The median grain size, $D_s \approx$ 1mm.

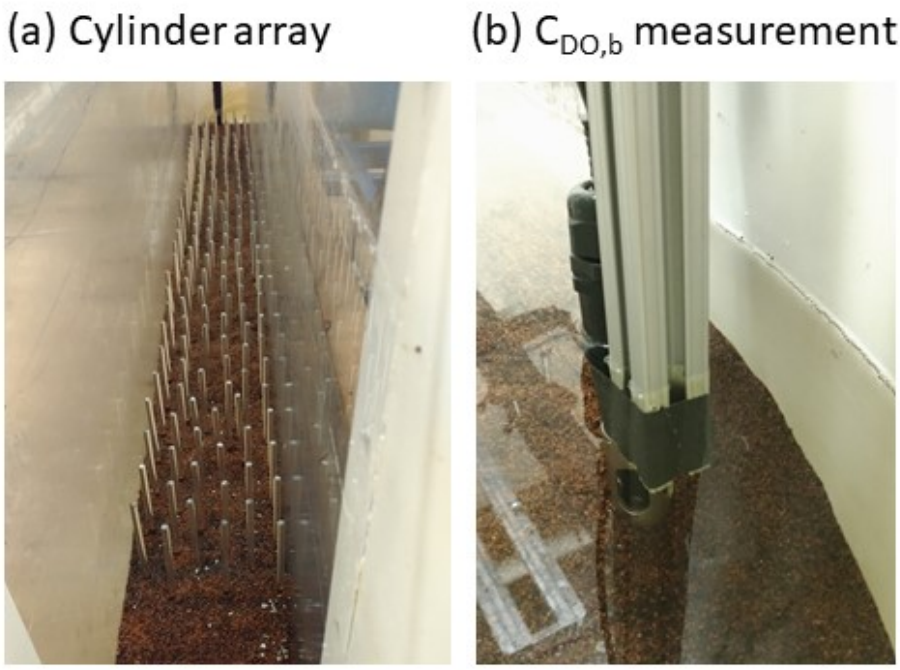

Figure 5. Experiment pictures of (a) the dense acrylic cylinder array (ah=0.5) with crushed walnut shells as the sediment substrate; (b) near-bed DO measurement by the optical PASCO DO sensor.

RESULTS

Flow Structures:

- Horizontal flow structures:

The horizontal flow structure validates the 2D vertical-plane approach in our thin flume, where wall effects can be ignored, even for the sparse and bare-bed cases. The result also shows that the velocity measured within the gap is representative of the velocity within the array.

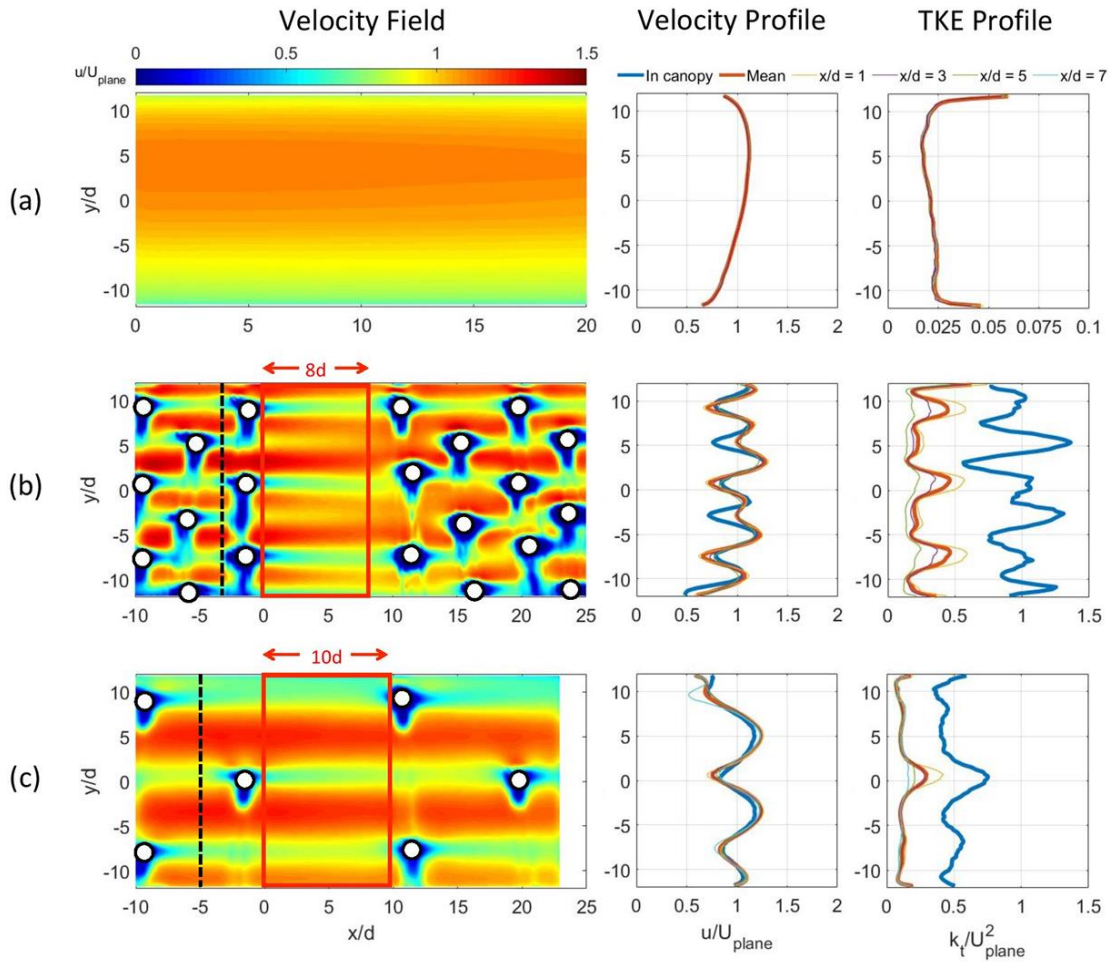

Figure 6. The horizontal plane-view 2D velocity field, velocity profile, and TKE profile measured by PIV at a horizontal plane 2 cm below the top of the canopy. The flume frequency, f, was 30 Hz under (a) bare-bed case (ah = 0.0), U_{plane} = 21.90 cm/s; (b) dense case (ah = 0.5), U_{plane} = 8.50 cm/s; (c) sparse case (ah = 0.1), U_{plane} = 14.82 cm/s. The white solid circles denote the locations of the vegetation. The red box in panel (b) and (c) show the observation window for each case, and Uplane is the plane-averaged velocity within the window as shown in Fig. 3 (a) and (c). The black dashed lines represent the locations where in-canopy profiles were measured.

- Vertical flow structures:

The velocity profiles on the sediment bed are similar to the velocity profiles on the smooth bed (Tseng and Tinoco 2020). The only difference can be found in the near-bed region where the sediment bed has a rougher boundary that results in a thicker boundary layer (the velocity reaches constant at higher z-location).

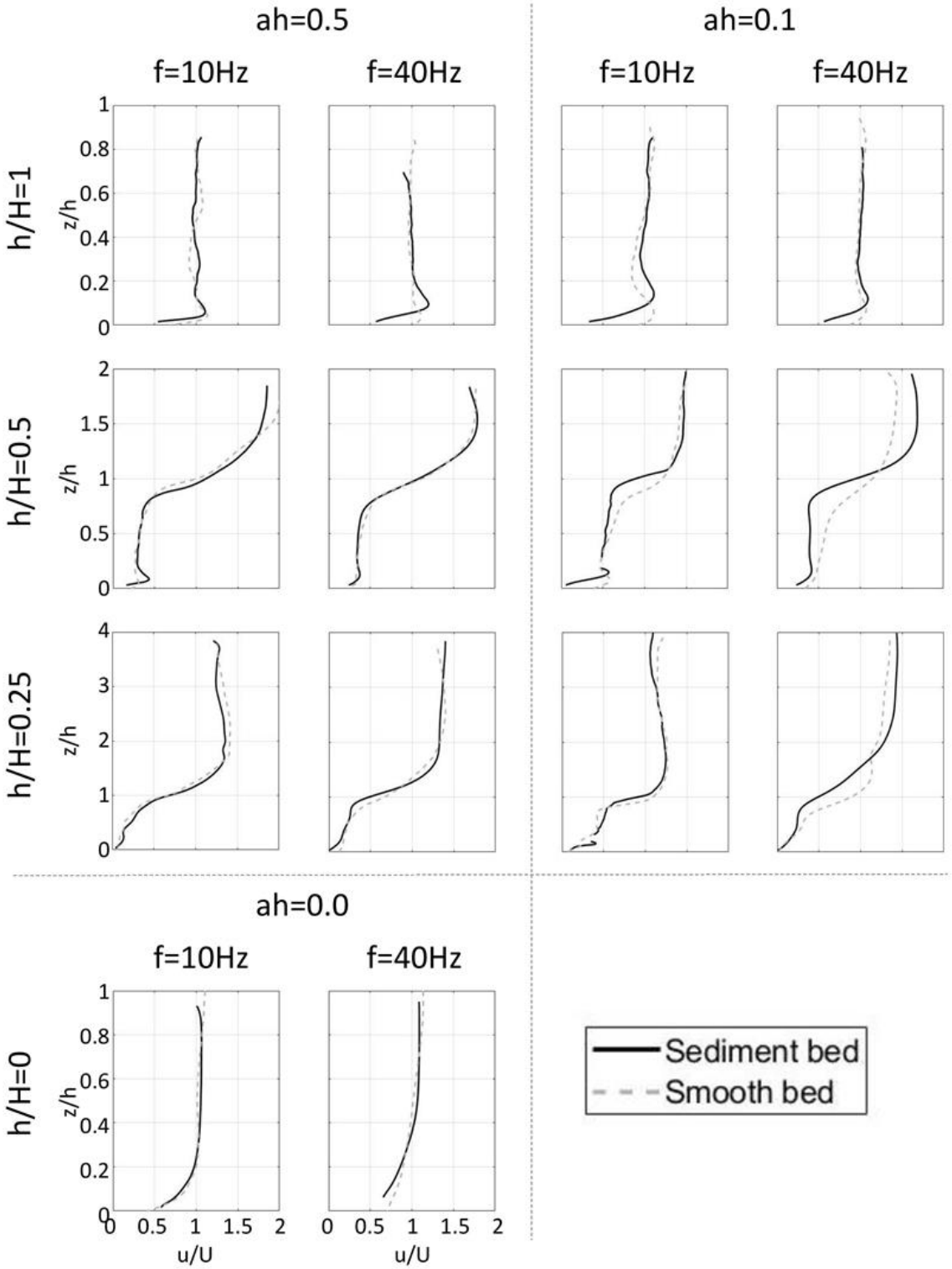

Figure 7. The normalized velocity profile under low flow (f = 10Hz) and high flow (f = 40Hz) velocity, different submergence ratios (h/H = 1, 0.5, 0.25, and 0), and different canopy density (ah = 0.5, 0.1, and 0). The black solid lines represent the experiment results with sediment bed compared with the grey dashed lines showing the data with the smooth bed (data from Tseng and Tinoco, 2020).

Like the TKE production profile on the smooth bed (Tseng and Tinoco 2020), the TKE production profile on the sediment bed also shows prominent features to connect mean flow rates to surface gas transfer rates.

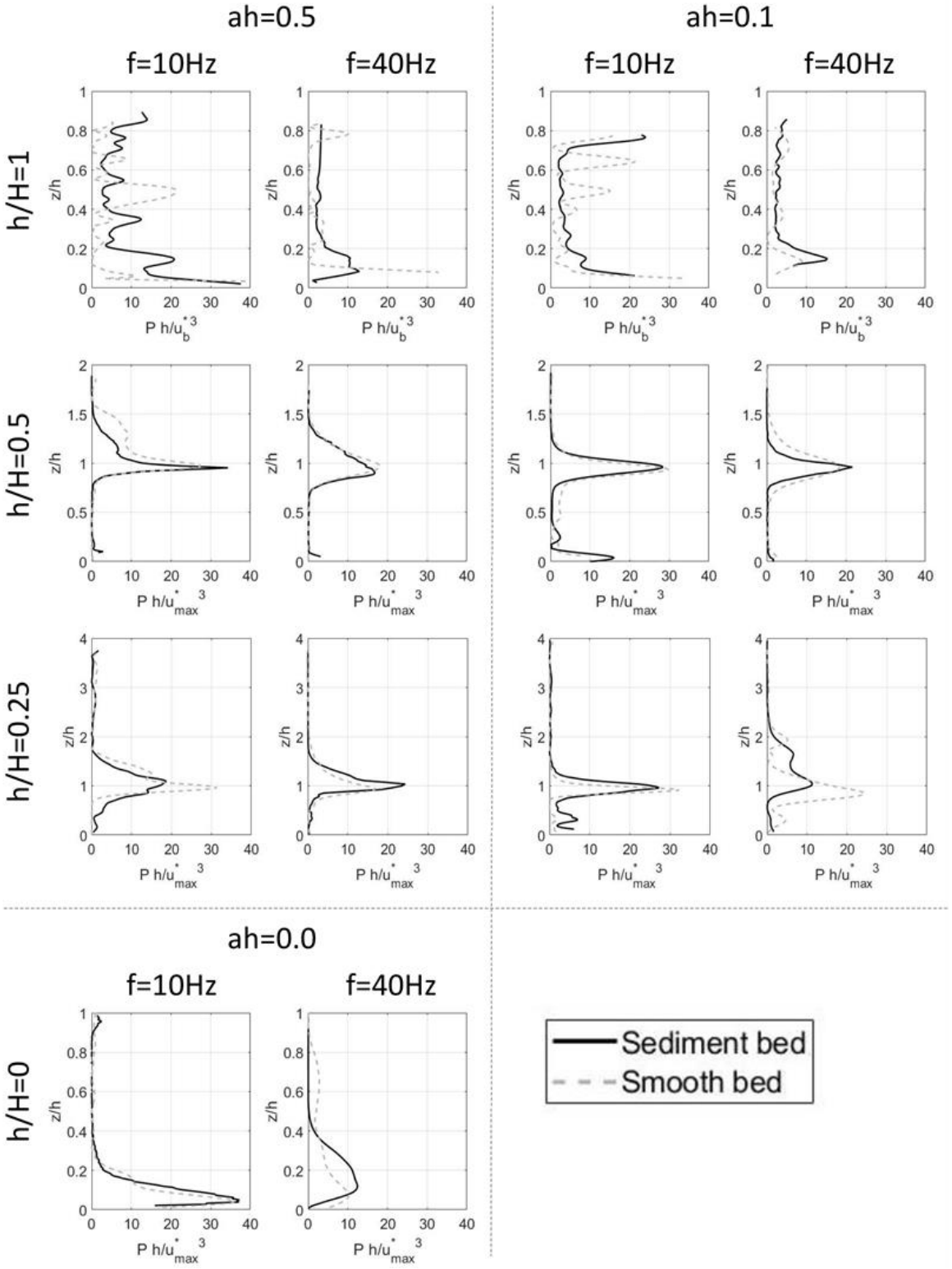

Figure 8. The normalized TKE production profile under low flow (f = 10Hz) and high flow (f = 40Hz) velocity, different submergence ratios (h/H = 1, 0.5, 0.25, and 0), and different canopy density (ah = 0.5, 0.1, and 0). The black solid lines represent the experiment results with sediment bed compared with the grey dashed lines showing the data with smooth bed (data from Tseng and Tinoco, 2020).

DO Re-aeration Curve:

The re-aeration process dominates the DO dynamics near the surface and the bed, but a delayed time can be observed in our cases, which can be obtained by fitting the curve according to Equation (6).

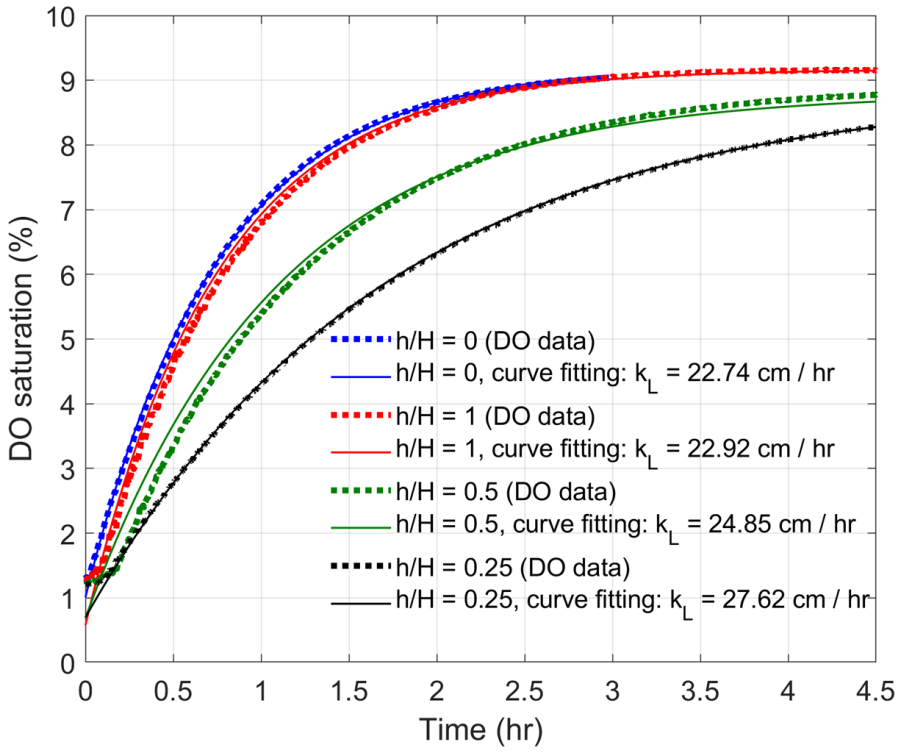

Figure 9. The fitting results of the gas transfer rate, k_L , based on equation (3) from DO measurements near the surface under flume frequency f = 30Hz with ah = 0.5 in different submergence ratios.

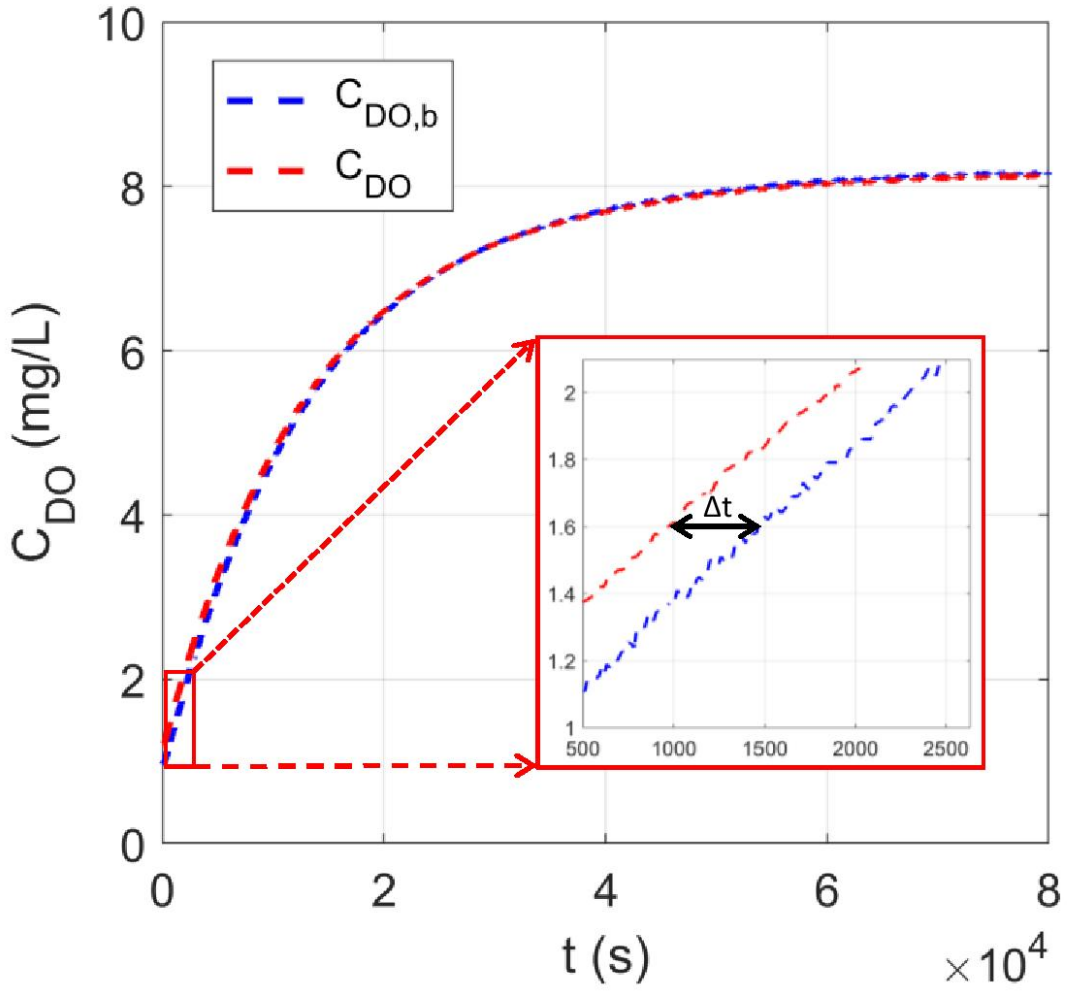

Figure 10. The re-aeration curves from DO measurements near the bed (blue dashed line) and the surface (red dashed line) under flume frequency f = 20Hz with ah = 0.1 and h/H = 0.25. The red subwindow shows the zoomed-in region of the beginning of the re-aeration process. A delayed time Δt can be observed from the difference between the two curves.

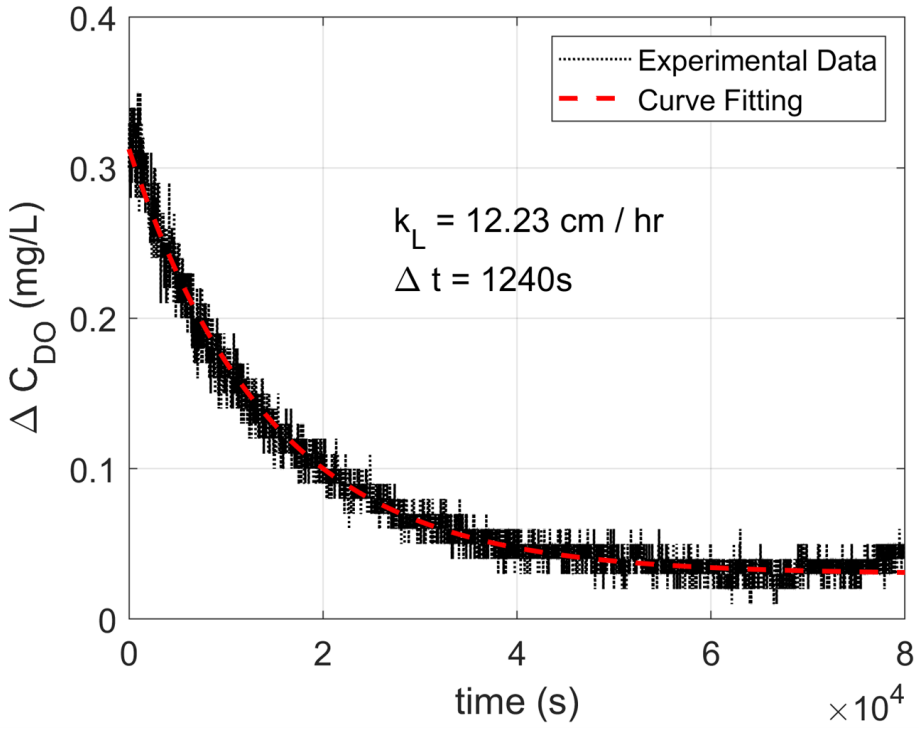

Figure 11. The fitting results of the delayed time, Δt , based on equation (6) and the fitted gas transfer rate, k_L , from equation (3) under flume frequency f = 20Hz with ah = 0.1 and h/H = 0.25.

DISCUSSIONS

Gas Transfer Rates:

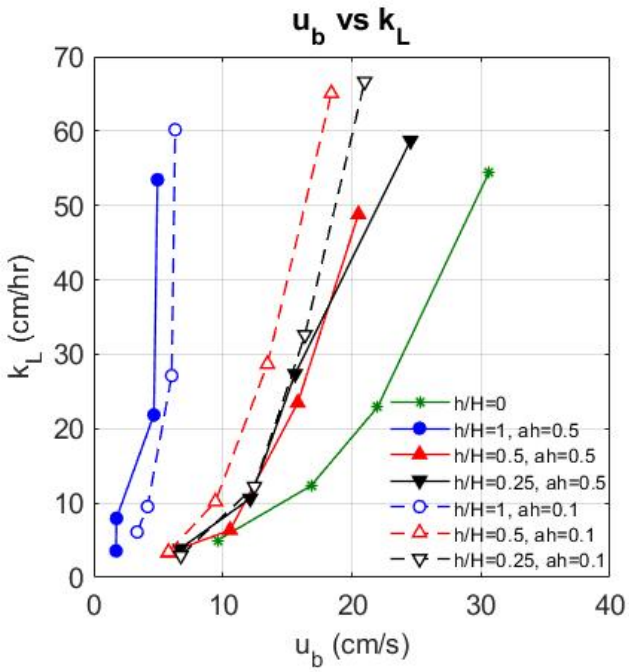

Figure 12. The relations between gas transfer rate, k_L, and the time-averaged bulk flow velocity, u_b, under different submergence ratios, h/H, and array roughness densities, ah. Solid and open symbols denote dense (ah = 0.5) and sparse (ah = 0.1) conditions, respectively.

The modified SR model proposed by Tseng and Tinoco (2020) works well to predict k_L in vegetated flows with the sediment bed.

General form: $k_L = \alpha\sqrt{L^+ P_c^{1/2} \frac{D}{\nu^{1/2}}}$

Emergent case: $P_c = P_b\,,\ L^+ = Re_d^{1/2} \frac{H^{1/2}}{d^{1/2}} \frac{u_b^{*1/2}}{u_b^{1/2}}$

Submerged case: $P_c = P_{max}\,,\ L^+ = Re_H^{1/2} \frac{L_{up}^{1/2}}{H^{1/2}} \frac{{u^*_{max}}^{1/2}}{u_b^{1/2}}$

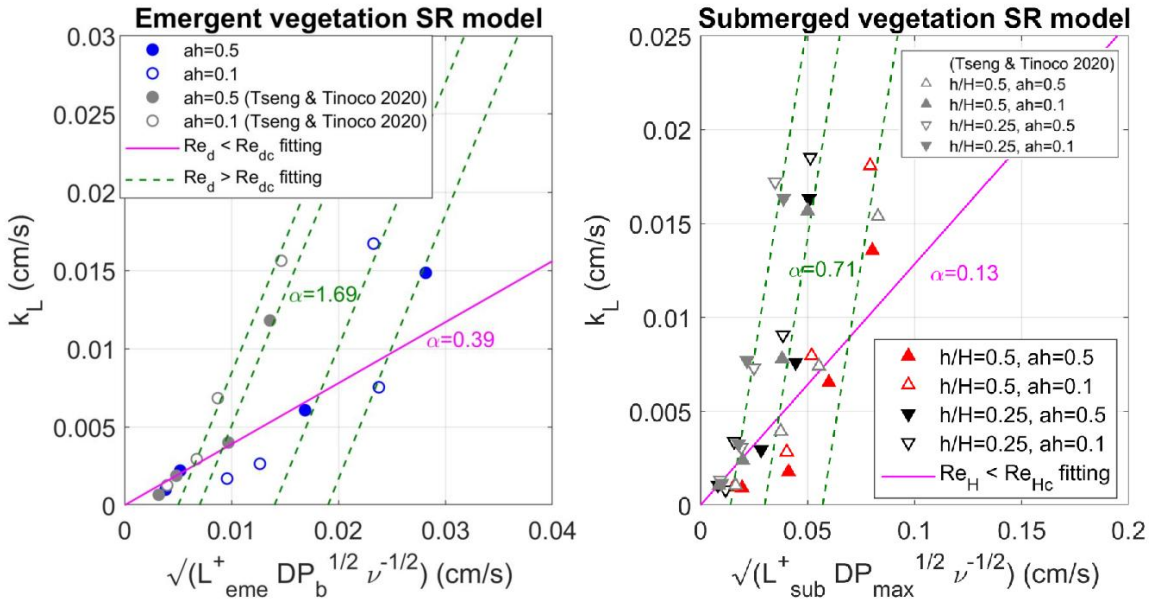

Figure 13. The linear fitting of the emergent (left) and submerged (right) canopy data by the modified SR model (Tseng and Tinoco 2020).

Sediment-Oxygen Flux:

The delayed time of re-aeration between the water and the near-bed region decreases as flow velocity increases. The curve varies with different submergence ratios, which clearly shows different mechanisms of the oxygen flux (J_{SOD}) from water to sediment.

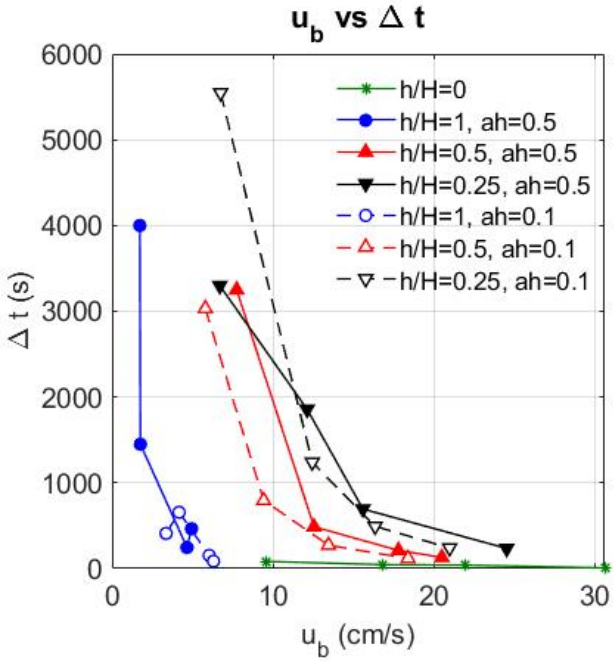

Figure 14. The relations of the delayed time, Δt, between the water and the near-bed region to the time-averaged bulk flow velocity, u_b, under different submergence ratios, h/H, and array roughness densities, ah. Solid and open symbols denote dense (ah = 0.5) and sparse (ah = 0.1) conditions, respectively.

SUMMARY AND ACKNOWLEDGEMENT

Summary:

- No geochemical effect from the organic sediment was observed during the re-aeration process.

- The modified SR model proposed by Tseng and Tinoco (2020) works well to fit the observed k_L in vegetated flows with the sediment bed.

- A delayed time of re-aeration between the water and the near-bed region was observed and varies with flow velocities and submergence ratios, which controls the oxygen flux (J_{SOD}) from water to sediment.

- Future studies are required to investigate the cause of the delayed time to incorporate sediment oxygen demand in a substrate-to-surface transfer model.

Acknowledgement:

- This study is supported by NSF through CAREER EAR 1753200. Any Opinions, findings and conclusions or recommendations expressed in this material are those of the authors and do not necessarily reflect those of the National Science Foundation.

- CT acknowledges funding support from Taiwan-UIUC Fellowship co-funded by Taiwan Ministry of Education and The University of Illinois at Urbana–Champaign.

AUTHOR INFORMATION

Chien-Yung Tseng
Ph.D. student, Department of Civil and Environmental Engineering, University of Illinois at Urbana-Champaign, Urbana, IL, USA
Email: cytseng2@illinois.edu
Website: https://jasonpig2001.wixsite.com/chienyung (https://jasonpig2001.wixsite.com/chienyung)

Rafael O. Tinoco
Assistant Professor, Department of Civil and Environmental Engineering, University of Illinois at Urbana-Champaign, Urbana, IL, USA
Email: tinoco@illinois.edu
Website: http://cee.illinois.edu/directory/profile/tinoco (http://cee.illinois.edu/directory/profile/tinoco)

ABSTRACT

Aquatic vegetation alters the hydrodynamics of natural waters, such as rivers, lakes, and estuaries. Plants can generate turbulence that propagates throughout the entire water column, which affects gas transfer mechanisms at both air-water and water-sediment interfaces, driving changes of dissolved oxygen (DO), an important indicator of water quality.

We conducted a series of laboratory experiments with rigid cylinder arrays to mimic vegetation using a staggered configuration in a recirculating race-track flume. Walnut shells were chosen as the sediment substrate, which interacts with DO in water. 2D planar Particle Image Velocimetry was used to characterize the flow field under various submergence ratios, highlighting the effect of vegetation on turbulence quantities. Gas transfer rates were determined by measuring the DO concentration during the re-aeration process based on the methodology proposed by the American Society of Civil Engineers.

Our data provide new insight on Air-Water-Vegetation-Sediment interactions in streams as a function of submergence ratio, array density, and flow turbulence. A modified surface renewal model using turbulence production as an indicator of gas transfer efficiency is used to predict surface gas transfer rates. A delayed time of re-aeration between the bulk and the near-bed region was observed and varies with flow velocities and submergence ratios, which controls the oxygen flux from water to sediment. Future studies are required to investigate the cause of the delayed time to incorporate sediment oxygen demand in a substrate-to-surface transfer model.

REFERENCES

1. Foster-Martinez, M., Variano, E.A., 2016. Airwater gas exchange by waving vegetation stems. Journal of Geophysical Research: Biogeo- sciences 121(7), 1916–1923.
2. Hondzo, M., & Nancy, S. 2008. Sediment oxygen demand (SOD) in rivers, lakes, and estuaries. In Sedimentation Engineering: Processes, Measurements, Modeling, and Practice (pp. 983–993).
3. Nepf, H.M., 2012. Flow and transport in regions with aquatic vegetation. Annual review of fluid mechanics 44, 123–142.
4. O'Connor, B. L., & Hondzo, M. 2008. Dissolved oxygen transfer to sediments by sweep and eject motions in aquatic environments. Limnology and Oceanography, 53(2), 566–578.
5. Poindexter, C.M., Variano, E.A., 2013. Gas exchange in wetlands with emergent vegetation: The effects of wind and thermal convection at the airwater interface. Journal of Geophysical Research: Biogeosciences 118(3), 1297–1306.
6. Tseng, C. Y., & Tinoco, R. O. (2020). A model to predict surface gas transfer rate in streams based on turbulence production by aquatic vegetation. Advances in Water Resources, 143, 103666.
7. Voermans, J. J., Ghisalberti, M., & Ivey, G. N. (2018). A model for mass transport across the sediment‐water interface. Water Resources Research, 54(4), 2799-2812.